ARTICLE

Photon and Fast Neutron Transmission Parameters of Metakaolin Doped Concrete

O.I. Olarinoye[1]   M.M. Idris[2*]   M. Kure[1]

1. Department of Physics, Federeal University of Technology, Minna, Nigeria
2. Department of Physics, Nasarawa State University, Keffi, Nigeria

ARTICLE INFO	ABSTRACT

Radiation-shielding properties of metakaolin doped concrete samples were investigated in this report. The gamma photon mass attenuation coefficients and exposure buildup factor of the samples were determined theoretically using WinXcom and EXABCal software respectively for the energy range of 15 keV - 15 MeV and fast neutron removal cross section for the concrete sample was evaluated. Results indicated that, oxides of silicon, aluminum, calcium and iron determined through the energy dispersive X-ray fluorescence spectrometric analysis constitute more than 85% of the chemical composition of the concrete samples. The oxides contribute 85.46, 86.47, 87.55, 88.75, and 86.15 % of the total chemical oxides in MK00, MK05, MK10, MK15, and MK20 respectively. Densities of the prepared MK doped concrete were in the range of 2.575-2.667 g/cm^3. Compressive stress of prepared MK doped concretes increased consistently with the curing period for each concrete sample. CS grew from 8.71 - 10.63, 8.84 - 10.83, 9.44 - 11.22, 10.89 - 11.53, and 10.76 - 11.43 MPa for MK00, MK05, MK10, MK15, and MK20 respectively as the period extends from 7 to 28 days. Mass attenuation coefficient decrease steadily with an increase in energy up to about 0.1 MeV and the decrease become smaller beyond this energy with increasing energy for all the mixtures. Fast neutron removal cross section results indicate that MK10 (0.07693 cm^{-1}) has the highest value of Σ_R followed by MK15 (0.07628 cm^{-1}) and MK20 (0.07537 cm^{-1}) while MK00 (0.07380 cm^{-1}) and MK05 (0.07404 cm^{-1}) have approximately the same value. It was found that MK10 concrete has the best gamma radiation and fast neutron shielding ability among the MK doped concrete under study.

1. Introduction

The continuous beneficial use of ionizing radiation (IR) and radioisotopes in the diagnosis and treatment of health trauma; electricity generation; food processing and preservation; material characterization and other peaceful purposes is hinged on adequate radiation protection of man

and the biota against the harmful effect of IR [1,2]. A commonly adopted radiation protection technique is the use of barrier (shield) to confine the IR to a restricted volume of space or attenuate the radiation to as low as acceptable outside the barrier. When there is no space and cost restraint, the use of concrete as structural shield is widely accepted in different areas of IR and radioisotope appli-

Corresponding Author:
M.M. Idris,
Department of Physics, Nasarawa State University, Keffi, Nigeria;
Email: idrismustapham@nsuk.edu.ng

cations [3-6]. Concretes can generally be produced with locally available materials into a wide variety of structural configurations while requiring very minimal maintenance during use. Reports on the IR shielding capacity of different types of concrete have been published by different research groups [2,4,7]. The conclusion drawn from most of these reports is that the radiation attenuating capacity of concrete is a function of the radiation properties (energy and type) and the concrete's physical and chemical properties. However, the physical and chemical properties of concrete is to a large extent dependent on the properties of its composition [2,5,6].

Traditionally, concrete is a mixture of binder (cement), aggregates (fine and coarse) and water. Of all these, cement is the most expensive per unit mass. Furthermore, the exploration of raw materials used in the production of cement and the production process causes environmental degradation and emission of CO_2 (a green-house gas) respectively [3,4]. In fact, the cement industry is one of the biggest emitters of green-house gases and other environmental pollutants [8]. These have made research investigating alternative materials with pozzolanic properties that could serve as cement replacement (fully or partially) in the production of concrete very active [2,3,5,8]. In radiation protection, such replacement must however, not reduce the mechanical strength and shielding capacity of the concrete [3,9].

Metakaolin (baked kaolin clay) is derived from the calcination of kaolin clay at a temperature between 600 and 900 °C [3,10]. Metakaolin (MK) is a pozzolanic material rich in silica and alumina and it reacts with calcium hydroxide to give compounds with cement-like properties [11]. The partial replacement of cement with MK in concrete has produced concrete with decreased porosity, increased density, higher resistance to water pressure and chemically aggressive environment, reduced aggregate segregation and bleeding, reduced shrinkage and improve the physical and chemical properties of concretes [11-14]. The partial replacement of MK in concrete has also been shown to decrease the radon exhalation rate in concrete [3,12,13].

The effect of partial MK replacement of cement in concrete on the photon and neutron shielding capacity of concrete is scarce in the literature. This study thus investigates the effect of partial replacement of cement by MK on the photon and fast neutron shielding capacity of concrete. Kaolin clay is a mineral found in large commercial quantity (circa 50 million metric tons in reserve) and much more untapped in different parts of Nigeria [15] and coupled with the fact that Nigeria is seriously considering the use of nuclear technology for electrical power generation are further motivations for this study.

2. Materials and Methods

2.1 Metakaolin and Concrete Production

Kaolin rocks obtained locally from *Alkeleri* area of *Bauchi* state, Nigeria were grounded into fine power to increase their surface area and improve homogeneity. The fine powder was subsequently calcined at 800 °C for one hour in an electric furnace. After this heat treatment the clay powder was air dried, grounded again and sieved through a 150 μm mesh sieve. The homogenized clay powder was then analyzed chemically and used for concrete production.

Ordinary portland cement, fine (FA) and coarse (CA) aggregates obtained locally together with water and produced metakaolin (MK) were used for concrete production. The aggregates conformed with the ASTM standard. Measured metakaolin and aggregates were dry mixed for about 300 seconds after which cement was added in the right proportion and mixed for another 270 seconds for consistence. Tap water was then added and the mixture was mixed for 2 minutes after which a polycarboxylate based superplasticizers was added and mixed for another 210 seconds. The design mix for the concrete cubes was 1:2:3 representing the ratio OPC: FA: CA while a water to cement ratio of 0.5 was adopted for all mixtures. The fresh mixtures were cast into a 50 x 50 x 50 mm steel moulds. By the use of a vibratory table with vibration time of 10 minutes, each concrete mould was added to give shape and reduce voids within the concrete matrix. The cubes were de-molded after 24 hours and put in curing tank filled with water at 20 °C for curing. In all, five mortar mixtures coded as MK00, MK05, MK10, MK15 and MK20 representing the partial replacements using MK by weight of cement (bwoc) at 0, 5, 10, 15 and 20% respectively were prepared.

2.2 Compressive Strength Determination

The curing period for the MK-concretes ranged from 7 to 28 days. For each of the curing period, the compressive strength of the concrete cubes was tested in triplicate according to the ASTMC109/C109M standard procedure [16]. The masses of the concrete sample were measured in order to determine their respective densities.

2.3 Chemical Analysis of Concrete Samples

The concentrations of major chemical oxides in the prepared concrete samples were determined through the energy dispersive X-ray fluorescence (EDXRF) spectrometric analysis. The concrete blocks were pulverised, sundried and continuously weighed after an interval of 24 hours until a

near constant weight was obtained. A portion (0.02 kg) of the pulverised and dried samples were mixed with a binder (PVC dissolved in toluene) carefully and pressed into circular pellets in a hydraulic press under a pressure of about 20 tons. The pellets each of diameter about 30 ± 3 mm were then put into the sample chamber of a PANanalytical Minipal4model PW4025/45B EDXRF spectrometer for chemical analysis of major oxides in the sampled concretes.

2.4 Calculation of Shielding Parameters

2.4.1 Photons

When a monochromatic beam of photons is incident on a thin absorbing medium of mass thickness t, the intensity upon emerging from the medium is evaluated using the equation:

$$I = I_o e^{-\mu_m t} \tag{1}$$

Where I, is the transmitted photon intensity while I_O and μ_m are respectively the incident photon intensity and the mass attenuation coefficient (MAC) of the material. The MAC is a measure of the mean number of photo-interactions which occurs between the incident photons and material medium of interest at a given mass thickness. It is a function of the energy of the incident photon.

$$\mu_m^c = \sum_i^n w_i (\mu_m)_i \tag{2}$$

In Equation 2, μ_m^c, is the mass attenuation coefficients of the composite material (concrete) while $(\mu_m)_i$ and w_i is the MAC of the ith component (oxide) in the concrete and its weight fraction respectively. The MAC values of the concrete samples were evaluated via the WinXCOM software. Using the obtained chemical composition of the concretes through the EDXRF analysis as shown in Table 1 as the input parameter in WinXCOM.

Many of the photon interaction processes depend on the atomic number (Z) of the interacting medium. A convenient parameter used to represent atomic number of multi elemental material such as concrete is effective atomic number. Z_{eff} is a function of energy as it varies with varying energy which is also It is an important parameter used for radiation dose measurement and shielding calculations [18,19]. The effective atomic number of the concrete samples were estimated using the equation [18,19]:

$$Z_{eff} = \frac{\sum_i f_i A_i (\mu_m)_i}{\sum_j f_j \frac{A_j}{Z_j} (\mu_m)_j} \tag{3}$$

Where f_i, A_i and Z_i are the fractional abundance, atomic weight and atomic number of element i.

When scattered and secondary photons within the material is transmitted, the right hand side of Equation 1 is usually corrected using a multiplying factor called photon buildup factor (B). The buildup factor depends transmit-

ting medium optical thickness, photon energy and detector response function among other factors. When the detector response function is the absorbed photon dose in air, the exposure buildup factor is prescribed. In this research, the exposure (EBF) buildup factors was considered and evaluated for the concrete samples using the EXABCal software [20] for different photon energies at selected depths.

2.5 Effective Removal Cross-Section of Fast Neutron

The attenuation of fast neutrons through a material medium can be estimated using its effective removal cross section. The fast neutron effective removal cross section Σ_R (FNRCS) is a measure of the likelihood that a neutron will undergo a given interaction per unit length of the material it transmits through. Σ_R has been developed to accommodate neutron scattering and buildup. For composite material, the Σ_R is often estimated via the equation [21-23]:

$$\Sigma_R = \bar{\rho} \sum w_i \left(\frac{\overline{\Sigma_R}}{\rho}\right)_i \tag{4}$$

Where, ρ, w_i, and $\left(\frac{\Sigma_R}{\rho}\right)_i$ is the mass density of the glass, weight fraction, and fast neutron mass removal cross section of the ith element in the absorbing/interacting material. $\frac{\Sigma_R}{\rho}$ is usually a smooth function of atomic number according to [21]:

$$\frac{\Sigma_R}{\rho} = 0.19 Z^{-0.743} \quad \text{for } Z \leq 8; \tag{5}$$

and,

$$\frac{\Sigma_R}{\rho} = 0.125 Z^{-0.565} \text{ for } Z > 8 \tag{6}$$

Σ_R of the concrete samples were estimated via Equations 4 - 6.

3. Results and Discussion

3.1 Compressive Stress

The obtained values of the compressive strength (CS) of the concrete samples as a function of curing period (in days) is depicted in Figure 1.

The figure shows a consistent increase in CS with the curing period for each concrete sample. CS grew from 8.71 - 10.63, 8.84 - 10.83, 9.44 - 11.22, 10.89 - 11.53, and 10.76 - 11.43 MPa for MK00, MK05, MK10, MK15, and MK20 respectively as the period extends from 7 to 28 days. For curing period above 7 days the CS of MK15 is the maximum compared to other concrete samples; and indicating that the optimum cement replacement level by MK which gives maximum CS is 15%. The increase in CS with metakaolin content increased could be attributed

to the increase in the oxides of silicon, aluminum, iron and calcium in the concrete samples. It is the reaction between these oxides that gives concrete the high stiffness and strength. Also, the stiffening and setting characteristics of cement paste primarily depend on hydration of aluminates [24]. The metakaolin content of the concrete though delay the concrete hardening process but increase the CS as MK content grows to an optimum level of 15%.
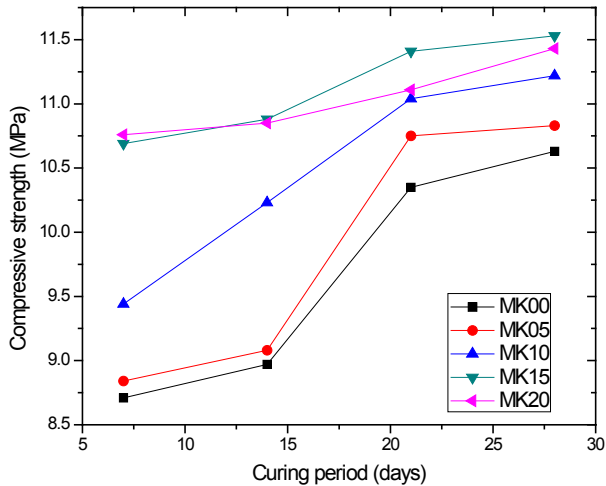
Figure 1. Compressive strength of the concrete samples as function of curing period.

3.2 Chemical Analysis of the Concretes

The result of the chemical (major oxides) analysis of the prepared concretes is given in Table1. The result shows that the oxides of silicon, aluminum, calcium and iron constitute more than 85% of the chemical composition of the concretes. These oxides to large extent dictate the chemical and mechanical features of the concrete. The oxides contribute 85.46, 86.47, 87.55, 88.75, and 86.15 % of the total chemical oxides in MK00, MK05, MK10, MK15, and MK20 respectively.

Also shown in Table 1 is the mass density (±0.001) calculated from the measured masses and volume of the concrete cubes. The density varied from 2.219 - 2.301 g/cm^3. The trend of the CS at 7-day curing period is similar to that of the density. Replacement of cement in concrete by MK up to 15% also increase the density of the concrete.

3.3 Photon Shielding Parameters

3.3.1 Mass Attenuation Coefficient

Calculated mass attenuation coefficient (MAC) (cm^2/g) of the MK-doped concretes for photon energies between 15 keV and 15 MeV and its variation with photon energy and MK replacement level is depicted in Figure 2.

Table 1. Chemical composition and mass density of concretes.

Oxides	Weighted fractions of samples				
	MK00	MK05	MK10	MK15	MK20
SiO_2	41.700	41.200	43.100	42.200	40.200
Al_2O_3	6.200	6.370	6.480	6.490	6.400
Na_2O	0.640	0.870	0.810	0.620	0.820
K_2O	0.460	0.840	0.442	0.442	0.042
CaO	36.060	37.400	36.900	38.430	38.280
MgO	2.030	2.000	1.880	1.900	2.040
TiO_2	0.220	0.310	0.250	0.300	0.290
Co_3O_4	0.010	0.010	0.019	0.004	0.010
Fe_2O_3	1.500	1.500	1.070	1.630	1.290
CuO	0.030	0.031	0.017	0.018	0.014
As_2O_3	0.006	0.010	0.008	0.007	0.006
SrO	0.450	0.510	0.037	0.440	0.440
ZrO_2	0.032	0.045	0.037	0.036	0.030
HfO_2	0.012	0.011	0.013	0.010	0.006
PbO	0.045	0.052	0.047	0.044	0.040
Density (g/cm^3)	2.219	2.248	2.301	2.274	2.261
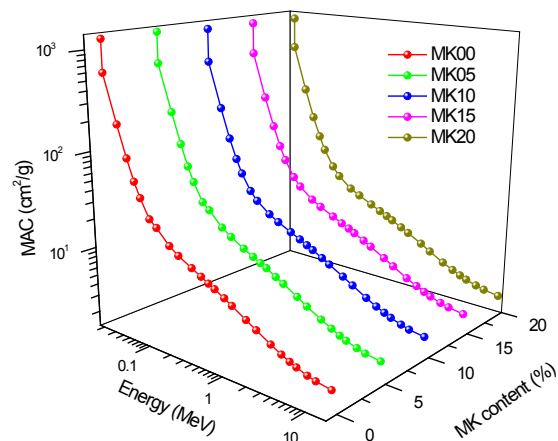
Figure 2. Mass attenuation coefficient (μ_m) of the MK doped concretes (MK0-MK20)

From Figure 2, the MAC value decrease steadily with increase in energy throughout the energy spectrum. However, the decline in MAC value was rapid for energies less than 150 keV compared to the remaining part of the energy spectrum. This rapid decline is due to the relatively high photoelectric interaction cross section (Σ_{PE}) at energies in the range $15 \leq E \leq 15$ keV since Σ_{PE} is proportional to E^{-4}. Beyond this energy range, the Compton scattering interaction dominates the photon interaction processes. The fact that cross section for Compton scattering (Σ_{CS}) is proportional to E^{-1} explains why the reduction in MAC values is less rapid for E >150 keV. Furthermore, a comparison between the MAC

values of the concretes reveals that MAC values range from 2.28 - 1256.89, 2.28 - 1265.36, 2.23 - 1164.72, 2.23 - 1169.72, and 2.11 - 1159.66 as energy varied from 15 keV - 15 MeV for MK00, MK05, MK10, MK15, and MK20 respectively. Obviously, the trend ($(MAC)_{MK20}$ < $(MAC)_{MK10}$ < $(MAC)_{MK15}$ < $(MAC)_{MK00}$ < $(MAC)_{MK05}$) is dictated by the chemical composition of the concretes. In the photoelectric interaction dominated energy region, the differences in the MAC values is higher than the Compton scattering dominated energies. This can be attributed to the dependence of Σ_{PE} and Σ_{CS} on the atomic number (Z) of the concrete. Typically, $\Sigma_{PE} \alpha Z^3$ while $\Sigma_{CS} Z$, hence the trend in the relative value of MAC could be the same with that of the effective atomic number of the concretes. Throughout the considered energy spectrum, MK05 had the highest MAC values an indication of the best photon absorber among the prepared concretes.

3.3.2 Effective atomic number

The Effective atomic number(Z_{eff}) of the MK doped concretes for 15 keV to 15 MeV photons as it varies with energy is shown in Figure 3. The Z_{eff} values were also noticed to lie between the minimum and maximum atomic numbers of the constituents elements. The largest values are seen in low - energy regions where the photoelectric absorption is the main interaction process. From 0.3 to 3 MeV the Z_{eff} values are reduced, this is the region where the Compton scattering is dominant. The lowest Z_{eff} can be noticed for photons of energy 1 MeV. Above 4 MeV, the Z_{eff} increases again after a period of being almost constant.
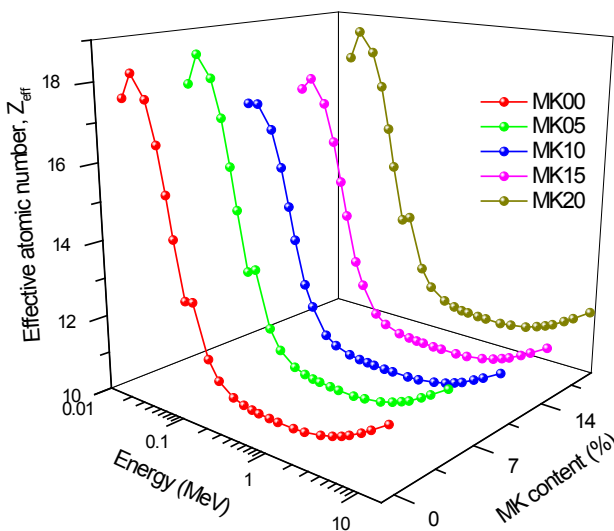
Figure 3. Effective atomic number (Z_{eff}) of the MK doped concrete (MK0-MK20).

3.4 The Exposure Buildup Factor

The Exposure Buildup Factor for mfp of 5, 10, 15, 20, 25 and 30 were calculated using the EXABCal software based on the GP fitting parameters. The energy variation of the incident photons for different mfp are presented in Figure 4(a-e).

Figure 4(a-e) presents the buildup factor changes with respect to energy and penetration depth. Irrespective of the material composition, EBF changes are similar with respect to energy. Thus, low values of EBF are observed at low energy and increases with increase in energy to certain maximum value. There is variation in peak of the plots as the material composition, energy of photon and depth of penetration varies. According to Olarinoye [9], these peaks range from 0.1 and 0.3 MeV for most materials. Beyond these peaks, a decrease in EBF is seen for all considered mfp with further increase in energy. Figure 5(a-e) the energy spectrum are categorized into low, intermediate and high energy region. This categorization is in accord with the three dominant photon interaction processes at the regions.

The photoelectric effect is the dominant mode of interaction at the lower end of the energy spectrum (15 keV - 0.1 MeV). For photoelectric effect, there is direct proportionality to the fifth power of the material's Z_{eq} and inverse proportionality to the third power of the energy under study. There is simply a removal of photons from the incoming beam thereby preventing buildup in this study. The EBF direct proportionality with Z_{eq} implies the higher Z_{eq} material will have a higher probability of removing photons than low Z_{eq} material. This is why the EBF of MK00 and MK05 are lower at these energies. The further increase in energy in the second region, the EBF is seen to increase with increasing energy. This dominated region by the compton interaction process is called the Compton region. The Compton interaction is directly proportional to the Z_{eq} at any given energy. The high EBF obtained at this region is because of the almost zero absorption taking place within this region. There is a mere degradation of photons in the process [9].

As the energy is increased further, a third interaction process kicks in. This interaction process begins at energies just beyond 1.022 MeV. Consequently, there is a decrease in EBF gradually with further increase in energy owing to the fact that the incident photons are utilized in pair production. Thus there is photons degradation in the process. Across Figure 4(a-e), is also worthy of note that higher mfp have higher EBF across the energy spectrum. This is because the EBF is a function of depth and thickness. The more the thickness, the more the chances
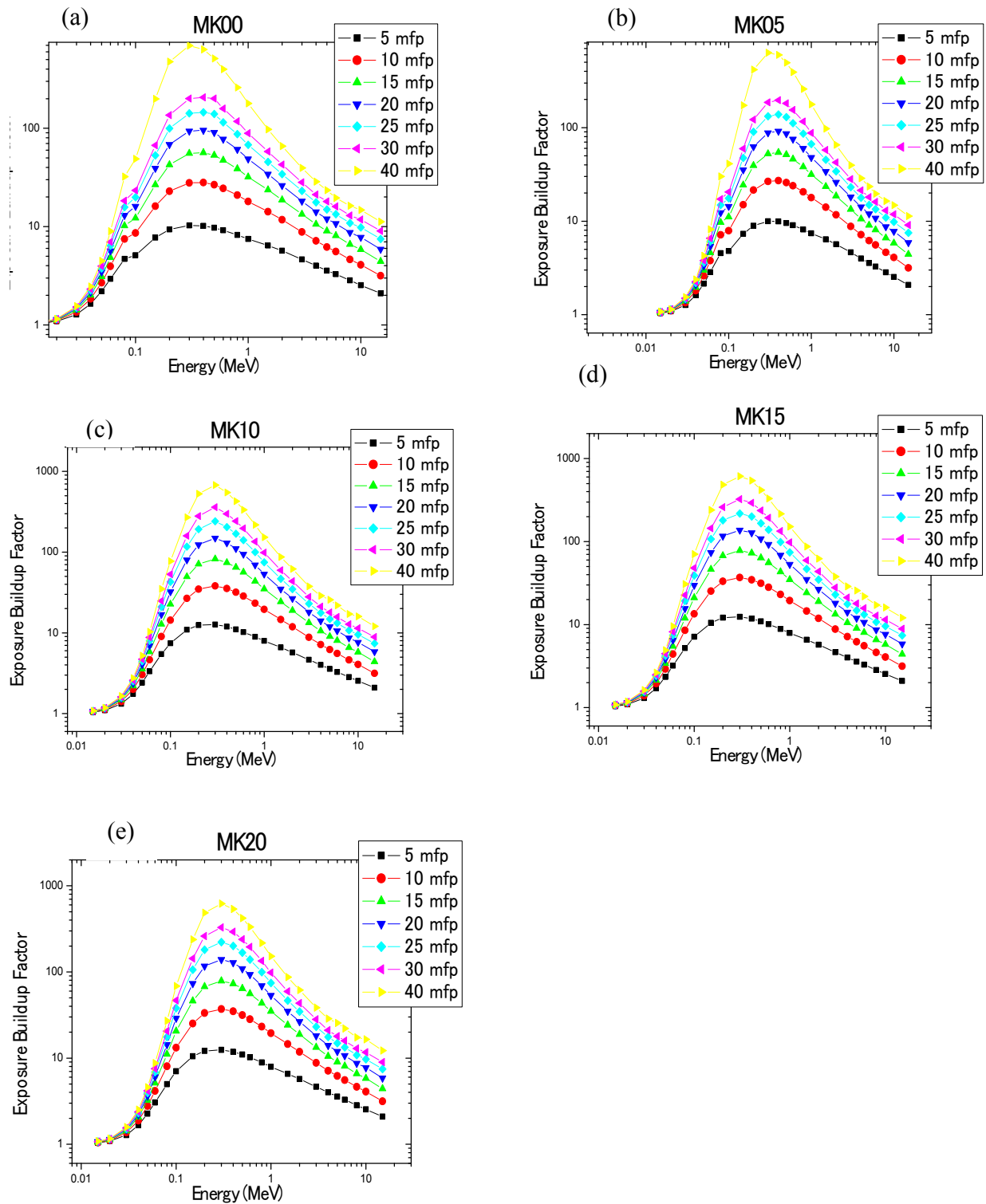
Figure 4. Energy Dependence and exposure buildup factors at various energy for MK doped concretes (MK0-MK15).

of having photons interaction which eventually escape the system. From Figure 4(a-e), 5 mfp has the least EBF while 30 mfp has the highest EBF as expected.

Exposure Buildup Factor Variation with Penetration Depth (mfp)

The variation of Exposure Buildup Factor with depths of the concretes are shown in Figure 5 (a - d) for the selected energies (0.015, 0.15, 1.5 and 15 MeV).

The EBF increases as the penetration depth increases. There is a rapid increase in EBF at lower depths for photon energy 0.015 MeV, and increases slightly as the mfp is increased for the materials under study. However, at 0.15 MeV photon energy, the increase is rather steady

with increase in energy. The lowest value of EBF was seen in MK05 followed closely by MK00. The MK10 has the highest value of EBF while MK10 and MK15 strongly overlapped between the highest and lowest EBF materials. At 1.5 and 15 MeV, the materials have similar variation in the value of EBF across all thicknesses. This account for the fact that at these energies, the Compton interaction process is dominant and hence across the thickness, they show a fairly constant value.

3.5 Fast Neutron Removal Cross Section

The Σ_R of the concretes was obtained through use of Equation 4. The variation of FNRCS with material is shown in Figure 6.
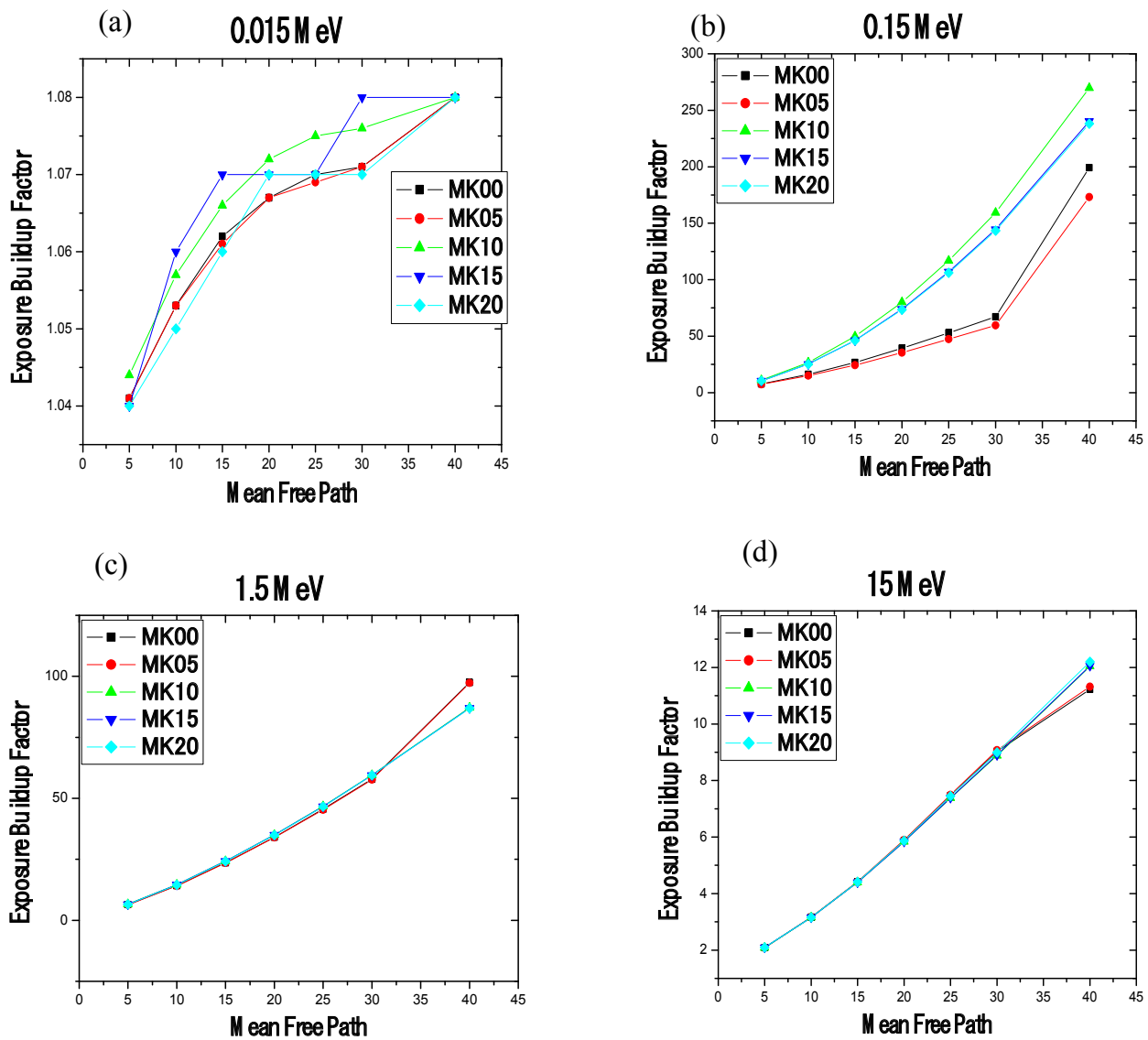
Figure 5. Variation of energy absorption buildup factor with the penetration depth for MK doped concretes (MK0-MK15).
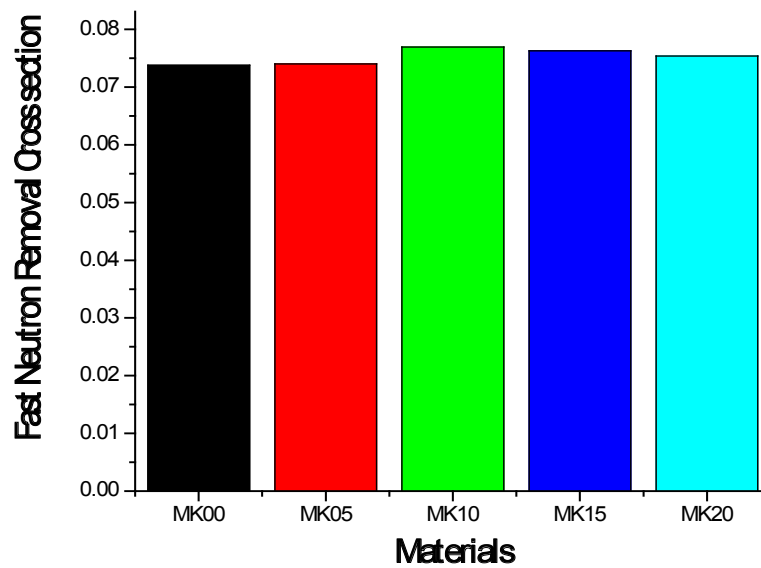
Figure 6. Fast Neutron Removal Cross Section for MK doped concrete (MK0-MK15).

The result showed that the Σ_R of MK00, MK05, MK10, MK15, MK20 were 0.07380, 0.07404, 0.07693, 0.07628, 0.07537 cm^{-1} respectively. MK10 have the highest value of Σ_R followed by MK15 and MK20 while MK00 and MK05 have approximately the same value. The closeness in their values can be attributed to their similar elemental composition. The higher values of Σ_R as seen in MK10, MK15 and MK20 can be attributed to the higher percentage of Carbon within their matrix compared to the other. The partial removal cross section of carbon is higher than every other element contained in the concretes considered. The two new BMG are thus good absorber for fast neutrons and are potentially better neutron shield material compare to heavy concretes.

4. Conclusions

In the current investigation, the mixture of metakaolin (MK), ordinary porland cement (OPC), coarse (CA), and fine aggregate (FA) were theoretically investigated. The densities of MK doped concrete were in the range of 2.575-2.667 g/cm^3. The mass attenuation coefficient of the MK concrete mixtures was investigated by the use of WinXCOM computer program at the orthovoltage and radiotherapy energies (15keV- 15MeV). Moreover, the neutron shielding features are calculated for the prepared MK doped concretes (MK00- MK20). The addition of metakaoline content has a significant effect to evolve the gamma shielding properties of the studied concretes. It was found that MK10 concrete has the best gamma radiation and fast neutron shielding ability among the MK doped concrete under study.

References

[1] Olarinoye I.O, El-Agawany FI, El-Adawy A., Rammah YS. Mechanical features, alpha particles, photon, proton, and neutron interaction parameters of TeO2-V2O3-MoO3 semiconductor glasses.
DOI: https://doi.org/10.1016/j.ceramint.2020.06.093.

[2] Hossaini M.S, Islma MAS., Quasem MA, Zaman MA, 2010. Study of shielding behavior of some multilayer shields containing PB and PX; *Indian journal of Pure and applied Physics*. 48, 860-868.

[3] Buket CÖ, Cavit ÇK, Banu O, Erkan G, Serdar A, 2020. Gamma and neutron attenuation properties of alkali-activated cement mortars, Radiation Physics and Chemistry. 166. 108478.
DOI: https://doi.org/10.1016/j.radphyschem.2019.108478

[4] Aycan G, Birol A, Tahir C, 2017. Photon Attenuation Properties Of Concretes Containing Magnetite And Limonite Ores; Physicochem. Probl. Miner. Process. 53(1), 184-191.

[5] Sabir BB, Wild S, Bai, J, 2001. Metakaolin and calcined clays as pozzolans for concrete: a review, *Cement and Concrete Composites*. 23(6): 441-454.

[6] Mohammad PI., Noor AM, Suhairy S, Abdul BM, Mohd KSS, Rahmad AR, 2001. Concrete mix design for X-and gamma shielding NDT group, Nuclear Malaysia.

[7] Ripan B, Hossaini S, Mollah AS, 2015. Calculation of gamma ray attenuation parameters for locally developed shielding materials: Polyboron; JRRAS, 9, 26-34

[8] Dunuweera SP, rajapakse RM, 2018. Cement types, composition, uses and advantages of nanocement, environmental impact on cement production and possible solutions.Advances in materials Science and Engineering.
DOI: https://doi.org/10.1155/2018/4158682.

[9] Olarinoye IO, 2017. Photon buildup factors for some tissues and phantom materials for penetration depths up to 100 MFP. J. Nucl. Res. Dev. 13, 57-67.

[10] Ženíšek Michal1, VLACH Tomáš, LAIBLOVÁ Lenka, 2016. Dosage of Metakaolin in High Performance Concrete; Key Engineering Materials.
DOI: https://doi.org/10.4028/www.scientific.net/KEM.722.311.

[11] Justice M. J, 2005. Evaluation of Metakaolins for use as supplementary cementitious materials; A thesis presented to school of civil and environmental engineering, Georgia Institute of technology.

[12] Lau B. M. F., R. V. Balendran and Yu K. N., 2003. Metakaolin As A Radon Retardant From Concrete; Radiation Protection Dosimetry TECHNICAL NOTE, Nuclear Technology Publishing. Vol. 103, No. 3, pp. 273-276.

[13] Sergio A., M. Avacir Casanova Andrello3, Marcos Antonio Scapin1, Sordi, Gian-Maria A. A., 2013. High density concrete to application in radiological protection. Asessement of the additions-microsilica-metakaolin-limestone filler. *International Nuclear Atlantic Conference - INAC 2013 Recife, PE, Brazil, November 24-29.*

[14] EL-Dakroury A.M., I.S. Ibrahium and I.E. Iyob, 2014. Development and performance properties of ternary mixed concrete; Arab Journal of Nuclear Science and Applications, 47(4), (27-39).

[15] Samuel A. O., 2012. Documentation, Application and utilization of clay minerals in Kaduna state (Nigeria); intechopen.com/books.
DOI: http://dx.doi.org/10.5772/48093.

[16] ASTMC109/C109M-16a, 2016. ASTMC109/C109M-16a: Standard Test Method for Compressive Strength of Hydraulic Cement Mortars (Using 2-in. or [50-mm] Cube Specimens).

[17] Gerward, L., Guilbert, N., Jensen, K.B. and Levring, H., 2004. WinXCom—a program for calculating X-ray attenuation coefficients. *Radiation physics and chemistry*, *71*(3-4), pp.653-654.

[18] Olarinoye, I., 2011. Variation of effective atomic numbers of some thermoluminescence and phantom materials with photon energies. *Res J Chem Sci*, *1*(2), pp.64-69.

[19] El-Mallawny, R., Sayyed, M.I., Dong, M.D., 2017. Comparative Shielding Properties of Some Tellurite Glasses. Journal of Non-Crystalline Solids.

[20] I.O. Olarinoye, R.I. Odiaga, S. Paul, 2019. EXAB-Cal: A program for calculating photon exposure and energy absorption buildup factors, Heliyon 5(7), e02017.

[21] Y.S. Rammah, I.O. Olarinoye, F.I. El-Agawany, El Sayed Yousef, S. Ibrahim, A.A. Ali, 2021. SrO-reinforced potassium sodium borophosphate bioactive glasses: Compositional, physical, spectral, structural properties and photon attenuation competence, Journal of Non- crystalline solids 559, 120667.
DOI: https://doi.org/10.1016/j.jnoncrysol.2021.120667.

[22] A. El-Khayatt, 2010. Calculation of fast neutron removal cross-sections for some compounds and materials, Annals of Nuclear Energy 37(2), 218-22.

[23] Schmidt, F. A., 1970. *Attenuation properties of concrete for shielding of neutrons of energy less than 15 MeV* (No. ORNL-RSIC-26). Oak Ridge National Lab., Tenn.

[24] Tanvir M., Nur Y., and. Abul B. E. Md, 2016. Potential of Carbon Nanotube Reinforced Cement Composites as Concrete Repair Material; Volume 2016, Article ID 1421959, 10 page.
DOI: http://dx.doi.org/10.1155/2016/1421959.